Ann. Geophys., 26, 709–724, 2008
www.ann-geophys.net/26/709/2008/

Annales Geophysicae

Structure of the near-Earth plasma sheet during tailward flows

A. Runov[1,*], I. Voronkov[2], Y. Asano[3], W. Baumjohann[1], M. Fujimoto[4], R. Nakamura[1], T. Takada[1], M. Volwerk[1,5], Z. Vörös[1,6], M. Meurant[2], A. Fazakerley[7], H. Rème[8], and A. Balogh[9]

[1]Space Research Institute, Austrian Academy of Sciences, 8042 Graz, Austria
[2]University of Calgary, Calgary, Canada
[3]Tokyo Institute of Technology, Tokyo, Japan
[4]Institute of Space and Astronautical Sciences, JAXA, Kanagawa, Japan
[5]Max Plank Institute for Extraterrestrial Physics, Garching, Germany
[6]Institute of Atmospheric Physics, Prague, Czech Republic
[7]Mullard Space Science Laboratory, UCL, London, UK
[8]Centre d'Etude Spatiale des Rayonnements, Toulouse, France
[9]Imperial College, London, UK
[*]now at: Institute of Geophysics and Planetary Physics, UCLA, Los Angeles, CA, USA

Received: 24 January 2007 – Revised: 26 February 2008 – Accepted: 3 March 2008 – Published: 26 March 2008

Abstract. A detailed analysis of successive tailward flow bursts in the near-Earth magnetotail ($X\sim-19\,R_E$) plasma sheet is performed on the basis of in-situ multi-point observations by the Cluster spacecraft on 15 September 2001. The tailward flows were detected during a northward IMF interval, 2.5 h after a substorm expansion. Each flow burst ($V_x<300$ km/s) was associated with local auroral activation. Enhancements of the parallel and anti-parallel ~1 keV electron flux were detected during the flows. The spacecraft configuration enables to monitor the neutral sheet ($B_x\approx0$) and the level of $B_x\approx10$–15 nT simultaneously, giving a possibility to distinguish between closed plasmoid-like structures and open NFTE-like surges. The data analysis shows NFTE-like structures and localized current filaments embedded into the tailward plasma flow. 3-D shapes of the structures were reconstructed using the four-point magnetic filed measurements and the particle data.

Keywords. Magnetospheric physics (Magnetotail; Plasma sheet)

1 Introduction

Several to ten minutes-long fast flows in the magnetotail, known as bursty bulk flows (BBFs, Angelopoulos et al., 1992), are observed to be predominantly Earthward in the near-Earth magnetotail (radial downtail distances $R<20\,R_E$) and mainly tailward beyond this distance (Nagai et al., 1998b; Baumjohann et al., 1999). Recent statistics of BBFs at the Cluster orbit ($R\sim19\,R_E$) shows that only 22% of the observed fast flows were tailward (Nakamura et al., 2004). These observations indicate that the fast flows are, most likely, generated by electromagnetic acceleration of plasma in the reconnection region usually located tailward of 20 R_E (e.g. Baumjohann et al., 1990; Nagai et al., 1998b). This process is the essential part of the Near-Earth Neutral Line (NENL) model of a substorm (e.g. Baker et al., 1996). In this context, tailward flows observed in the near-Earth magnetotail seem intriguing. Their appearance implies either enhanced magnetic activity (e.g. Miyashita et al., 2005; Nagai et al., 2005) or a mechanism that differs from acceleration at a NENL (e.g. Schödel et al., 2001).

Magnetic reconnection (MR) is, generally, a change of the magnetic field topology with magnetic field X-line formation and plasma acceleration via the magnetic tension force in the vicinity of X-line. The bulk outflows resulting from MR carry the oppositely directed magnetic field loops: The magnetic field is directed northward within the Earthward outflow and southward within the tailward outflow. One of the predictions of the NENL model, is the formation of a magnetic field structure, known as a plasmoid (e.g. Hones, 1979). Although both tailward and Earthward traveling plasmoid-like structure were observed (e.g. Zong et al., 2004), the term "plasmoid" is usually used for closed magnetic structures (magnetic islands), manifested as the north-south bipolar variation of the magnetic field, embedded into tailward bulk flow (e.g. Mukai et al., 1996; Ieda et al., 1998).

Correspondence to: A. Runov
(arunov@igpp.ucla.edu)

Published by Copernicus Publications on behalf of the European Geosciences Union.

Plasmoid-related tailward flows were found to be almost always associated with auroral breakups or pseudo-breakups (Ieda et al., 2001; Nakamura et al., 2001).

The presence of even a small cross-tail magnetic field component (B_y) leads to an appearance of a more complex 3-D structure, called "flux rope" (e.g. Slavin et al., 2003), instead of a 2-D magnetic loop, with the B_y sign correlating with that in the IMF. It was also found in simulations that a strong B_y component, or core-field, may be generated in the course of plasmoid evolution (Hesse et al., 1996). Alternatively, a large B_y may be generated due to localized reconnection of sheared magnetic fields (Shirataka et al., 2006).

The energetic electrons, generated in the course of MR (e.g. Hoshino et al., 2001), may be used to probe the magnetic field structure. They provide information about changes in the open and closed magnetic field line configuration. Particularly, the observation of the enhanced electron flux in association with the magnetic field bipolar variation was interpreted as the indication of the closed O-type magnetic structure (Zong et al., 2004).

The bipolar variation of the magnetic field may be explained in the frame of so called Nightside Flux Transfer Events (NFTE, Sergeev et al., 1992, 2005) – a magnetic surge in the magnetotail plasma sheet containing accelerated plasma, generated by a reconnection pulse. Contrary to a plasmoid, NFTE implies a locally open magnetic field structure. The bipolar variation in the NFTE case is asymmetric: the flow burst predominantly carries the unipolar magnetic field (southward in the case of a tailward flow). A turn to another polarity, observed above and below the neutral sheet, is due to the magnetic field compression by the flow. A spacecraft crossing the NFTE related magnetic loop near the neutral sheet will detect a unipolar variation. Numerical simulations show that, at early stage, a plasmoid may have a structure, locally open at the tailward side, resembling NFTE (Abe and Hoshino, 2001).

Theoretical models of fast pulsed reconnection, resulting in NFTEs, predict formation of a pair of slow shocks, separating inflow and outflow regions (e.g., Petschek, 1964; Semenov et al., 2004). The slow shocks were observed in the distant tail ($X<-100\,R_E$) on the lobe-plasma sheet boundary (e.g. Saito et al., 1995) and on the plasmoid boundaries at $X\sim-100\,R_E$ (Mukai et al., 1996). Recently, Eriksson et al. (2004) reported observations of reconnection related shocks in the near-Earth tail. The shear stress balance (Walén test, e.g. Khrabrov and Sonnerup, 1998) at fast flows, implying plasma acceleration by magnetic tension and predicting near-Alfvénic velocity of the accelerated plasma in the de Hoffmann-Teller reference frame, was considered as evidence of reconnection on the magnetopause (Paschmann et al., 1979; Sonnerup et al., 1981; Paschmann et al., 1986) and in the magnetotail (Øieroset et al., 2000; Eriksson et al., 2004).

The observations of tailward flows in the near-Earth magnetotail, discussed in literature, attribute the flows to near-Earth reconnection (e.g. Sergeev et al., 1995; Nagai et al., 1998a; Miyashita et al., 2005). Alternative hypotheses of a near-Earth flow onset are based on the current disruption (CD) concept (e.g. Lui, 1996). The CD framework is based on an idea of local decrease of the cross-tail current in the near-Earth magnetotail at -8 to $-12\,R_E$ due to development of instability after near-Earth current sheet thinning down to a critical thickness. (see Lui, 2004, for a review). The resulting inductive electric field leads to the drift motion of plasma. This model predicts strong "turbulent" fluctuations of the magnetic field ($\delta B\sim B$), ion energization perpendicular to the magnetic field and field-aligned electron beams (Lui, 1996). Southward magnetic field tailward of CD, produced by local generation of dawnward current, may lead to tailward bulk flow (Lui et al., 2006). Another possible mechanism of the near-Earth CD involves a development of the ballooning instability at the inner edge of the plasma sheet (Roux et al., 1991; Voronkov, 2005; Roux et al., 2006). This model predicts quasi-periodic variations of the magnetic field with the azimuthal wave number $k_y \gg (k_x, k_z)$. The tailward plasma flow is due to electric drift. The CD region expands tailward at a speed of 200–300 km/s (Ohtani et al., 1992) as a front of the magnetic field dipolarization. The turbulent CD-related tailward flow does not contain a plasmoid-like magnetic structure or any orderly magnetic field pattern (Lui et al., 2006). The $\mathbf{j}\times\mathbf{B}$-force components are expected to be rather chaotic within a plasma flow due to the turbulent CD. The ballooning-based CD apparently can produce a more regular magnetic structure.

In this paper we discuss in situ Cluster observations of a set of successive tailward flow bursts in the near-Earth magnetotail plasma sheet during 03:30–04:30 UT on 15 September 2001. The measurements at four probes, forming the tetrahedron with the scale <2000 km, give the possibility to identify spatial structures with scales comparable or larger than the probes separation and discriminate between plasmoid-like structures, NFTEs, and waves. Furthermore, four-point magnetic field measurements enable the estimation of the magnetic field gradient and magnetic tension inside the flows, which may help to understand the process of their formation.

2 Instrumentation

For the analysis of the tailward flows, observed by Cluster at $X\sim-19\,R_E$, we use magnetic field data from Cluster Flux Gate Magnetometer (FGM, Balogh et al., 2001), ion data from the Cluster Ion Spectrometry (CIS, Rème et al., 2001) experiment and electron data from the Plasma Electron And Current Experiment (PEACE, Johnstone et al., 1997). The ion data are provided by Cluster 1 and 3 (called C1 and C3 further on) Hot Ion Analyzer (HIA), with energy range ~5 eV/e–32 keV/e, and the Composition Distribution Function (CODIF) instrument with energy range 20–40 keV/e and by the Cluster 4 (C4) CODIF instrument. No ion data are

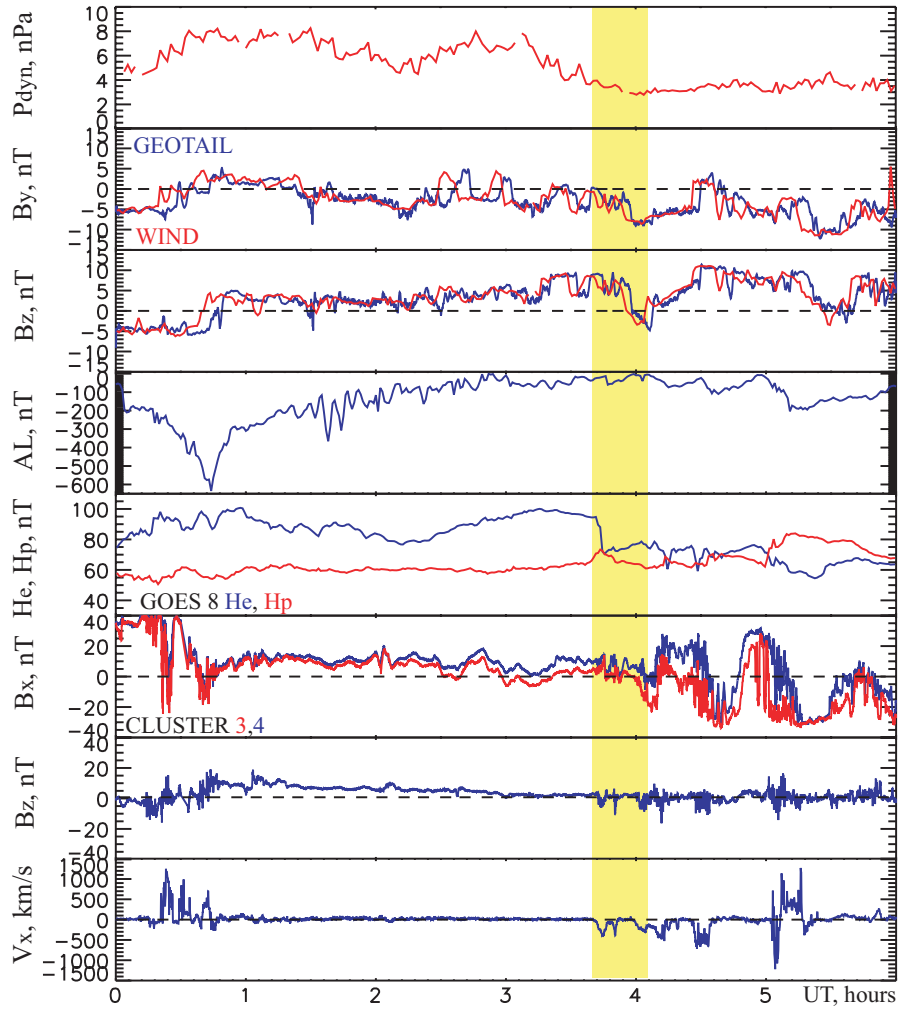

Fig. 1. Solar wind dynamic pressure, IMF B_y and B_z, AL-index, magnetic field at geostationary orbit, magnetic field (B_x and B_z) and ion bulk velocity (V_x) observed by C4 (blue) and C3 (red) in the magnetotail during 00:00–06:00 UT on 15 September 2001. GSM coordinate system is used for the vector components.

provided by Cluster 2 (C2). The PEACE instrument enables the measurement of the electron flux with energy 10 eV–26.5 keV; the PEACE data are provided by all four spacecraft. The telemetry transmission worked in the burst mode from 00:30 till 04:30 UT during the event discussed below, providing one ion and one electron distribution functions per spacecraft spin (~4 s), and the magnetic field with maximum time resolution is 67 Hz.

3 Event description

Figure 1 presents an overview plot of the interplanetary media, and the magnetosphere state history during 00:00–06:00 UT on 15 September 2001: The solar wind dynamic pressure $P_{\rm dyn}$ at the WIND satellite orbit ([53.5, −38.9, 19.4] R_E, GSM, at 04:00 UT), IMF B_y and B_z at Geotail ([9.1, −14.9, 4.4] R_E, GSM, at 04:00 UT) and WIND satellites, AL-index from the Kyoto monitor, H_e and H_p magnetic field components at geostationary orbit, X- and Z-components of the magnetic field and the X-component of the ion bulk velocity in the magnetotail from the Cluster spacecraft. The GSM coordinate system is used throughout this paper. The substorm during 00:00–01:00 UT was associated with a southward IMF and Earthward bursty bulk flow, detected by Cluster. At ~00:50 UT, B_z at Geotail turned northward and stayed predominantly northward, fluctuating between 0 and 10 nT during several hours, with several short turns southward after 03:40 UT. IMF B_y at Geotail and WIND showed similar variations with lag time of 5 min. The solar wind dynamic pressure ($P_{\rm dyn}$) decreased gradually from 8 down to 3 nPa during 03:00–04:00 UT. AL increased to zero at about 02:50 UT. A gradual increase of the H_e-component was observed by GOES 8 at geostationary orbit

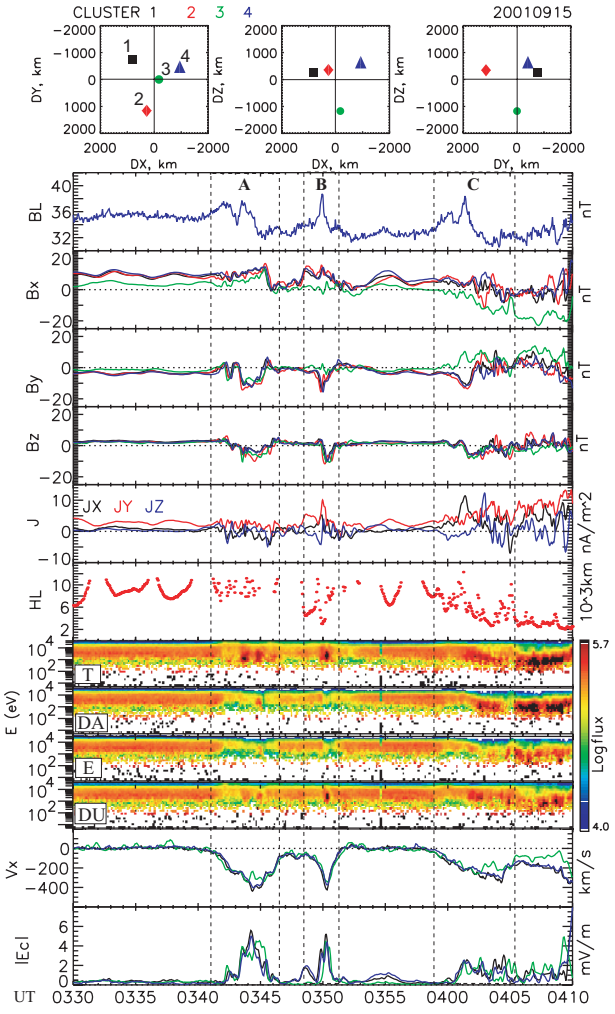

Fig. 2. Cluster spacecraft configuration and Cluster observations during 03:30–04:10 UT on 15 September 2001. From top to bottom: The lobe magnetic field strength (BL), estimated assuming pressure balance; X,Y, and Z GSM components of the magnetic field from C1 (black), C2 (red), C3 (green) and C4 (blue); X,Y, and Z GSM components of the electric current, The Harris estimate of the current sheet half-thickness; Ion time-energy spectrograms from C3 HIA for tailward (T), dawnward (DA), Earthward (E), and duskward (DU) streaming sectors separately; Ion bulk velocities at C1, C3 and C4; The convective electric field $E_c = -\mathbf{V}\times\mathbf{B}$ (absolute value).

during ~02:30–03:40 UT. Staying in the magnetotail plasma sheet ($|B_x|<20$ nT) during 01:00–03:40 UT, Cluster detected a gradually increasing magnetic field gradient (difference between B_x at C3 and C4, separated mainly along Z) with negligible ion bulk velocity. B_z gradually decreased during 01:00–03:30 UT. A set of bursty tailward flows were detected by Cluster/CIS between 03:40–04:40 UT. The frequency and amplitude of the magnetic field fluctuations increase during the flows in comparison with those during 01:00–03:40 UT.

A drop of H_e from ~100 down to 70 nT with a simultaneous increase of H_p was observed by GOES 8 at the onset of the first flow burst (03:41 UT). IMF B_z at Geotail and WIND was positive (~10 nT). A set of jump-like variations in B_y and B_z IMF were detected by WIND and Geotail between 03:20–03:40 UT. Some minor activations (with $|AL|<100$ nT) correspond to the flow bursts. Distinct auroral activations (pseudo-breakups and small substorms), corresponding to the tailward flow bursts observed in the plasma sheet, were detected by the CANOPUS stations (not shown, see Voronkov et al., 2006, for detailed description and timing) and the IMAGE satellite.

Further in this paper we will discuss the Cluster measurements during the three tailward flows observed between 03:40–04:07 UT (highlited interval in Fig. 1). The state of the magnetosphere is changed rapidly at about 04:07 UT (Voronkov et al., 2006). This change is, most likely, triggered by short southward IMF turn, detected by WIND and Geotail at about 04:00 UT (see Fig. 1). The two intensive tailward flows at 04:10 and at 04:25 UT, as well as the flow reversal at about 05:10 UT, studied by Xiao et al. (2006), are associated with substorm signatures, while the less intensive flow bursts during 03:40–04:07 UT correspond to rather pseudo-breakup activations (Voronkov et al., 2006).

During 03:30–04:10 UT Cluster stayed in the magnetotail plasma sheet at $[-18.9, 3.4, -3.1]$ R_E (barycenter), forming a nearly regular tetrahedron with the largest inter-spacecraft distance of 1750 km. Figure 2 presents the spacecraft configuration with respect to the tetrahedron barycenter and the summary plot of the Cluster observations during this interval. The intervals corresponding to the three distinct successive tailward flow bursts, detected by Cluster, are marked A, B, and C, respectively. Figure 3 presents IMAGE-WIC aurora observations, corresponding to the three intervals.

Before the first tailward flow was detected at 03:41 UT, plasma sheet was quiet (no ion velocity exceeding 50 km/s was observed, Fig.2) and relatively hot, with ion energy ~10 keV. The magnetic gradient in the current sheet was directed along Z (B_x at C3 was smaller than that at the other three spacecraft), $j_y > (j_x, j_z)$. The current sheet half-thickness, estimated using the Harris function (Harris, 1962), varied between 1–2 R_E (6000–10 000 km).

The ion energy increased between 03:41–03:51 UT and between 03:59–04:06 UT, somewhat exceeding the energy range of the CIS instrument (40 keV). Ion energy-time (ET) spectrograms show clear anisotropy of the ion flux during these intervals: The flux of the tailward (T) streaming ions is larger than that of Earthward streaming ions, indicating tailward ion bulk flow between 03:41–03:47 UT (A), 03:49–03:52 UT (B), and 03:59–04:06 UT (C). The lobe magnetic field value locally increased and then decreased during these intervals. Each tailward flow burst was associated with large-scale (several minutes, 5–20 nT) variations of the magnetic field and with increase of the magnetic field small scale fluctuations (10–200 s, several nT). In average, all three tailward

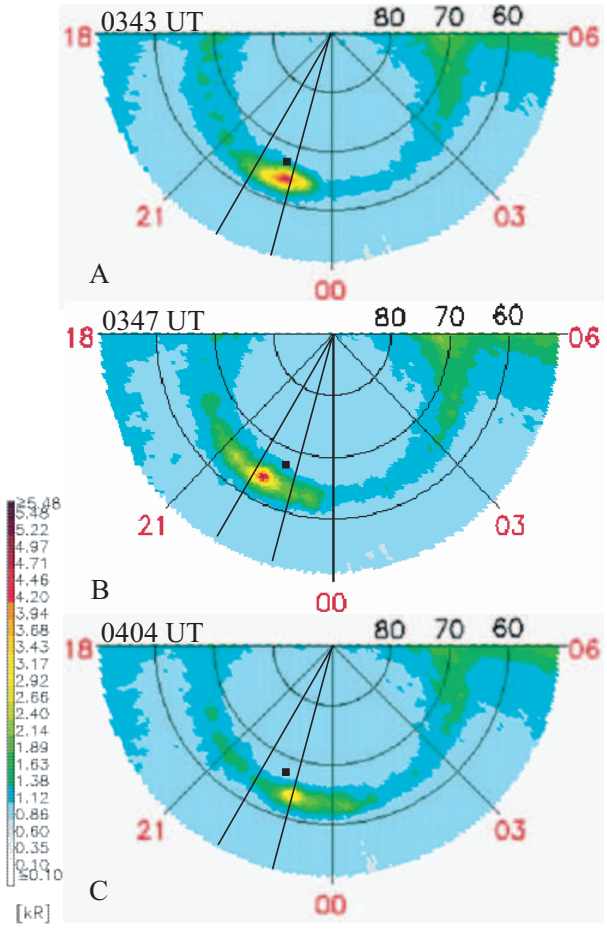

Fig. 3. IMAGE WIC snapshots at onsets of the auroral activation corresponding to the three tailward flows (*A*, *B*, and *C*) detected by Cluster between 03:40–04:10 UT. Cluster foot points (T89) are marked by black squares.

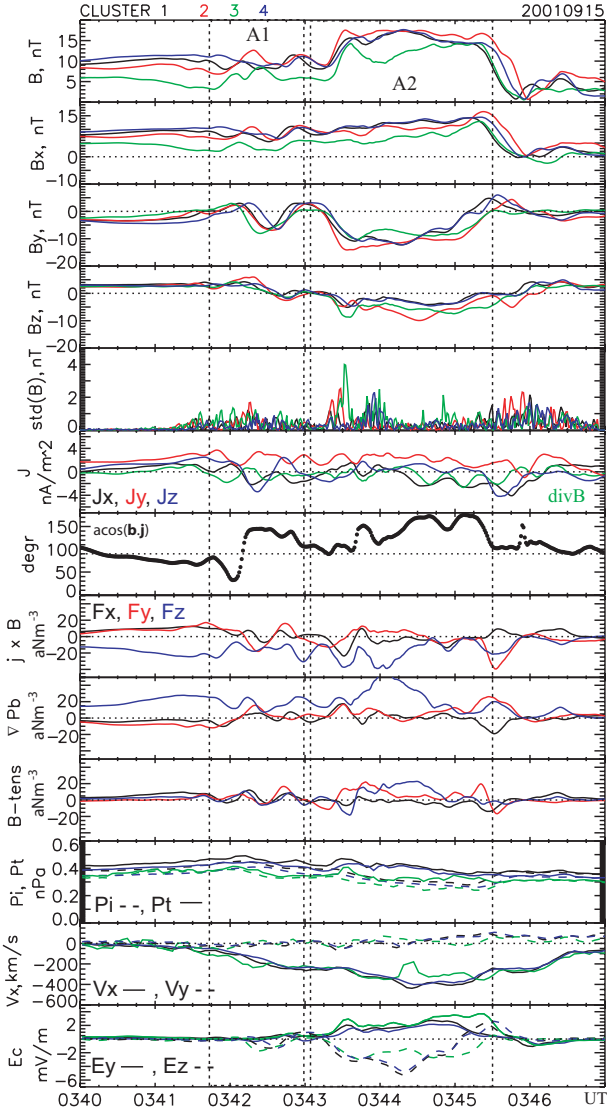

Fig. 4. Cluster observation during interval *A*. From top to bottom: Magnetic field magnitude; *X*, *Y*, and *Z* components of the magnetic field at the four spacecraft; standard deviation of *B*; *X*, *Y*, and *Z* components of the electric current density $\mathbf{j}=\mu_0^{-1}\nabla\times\mathbf{B}$; The angle between **j** and **B**; *X*, *Y*, and *Z* components of the $\mathbf{j}\times\mathbf{B}$ force, magnetic pressure gradient and magnetic field tensions; ion and total pressures; *X* and *Y* components of the ion bulk velocity; and *Y* and *Z* components of the $\mathbf{E_c}=-\mathbf{V}\times\mathbf{B}$ electric field. The GSM coordinate system is used for vectors.

flow bursts correspond to negative variation of B_z. Variations of B_y were up to ∼20 nT, and negative in the northern half of the current sheet ($B_x>0$) and positive in the southern one ($B_x<0$). The current density, derived from four-point magnetic field measurements (e.g. Chanteur, 1998), increased during intervals *B* and *C* up to $j\sim10$ nA/m^2 from $j\sim3$–5 nA/m^2 before the flow onsets, but fluctuated around ∼4 nA/m^2 during interval *A*. j_y remained positive, indicating a constant presence of the cross-tail current during the flow bursts; j_x and j_z showed large-amplitude variations (up to 10 nA/m^2, often with sign change), manifesting a complex, 3-D structure of the magnetic field within the flow bursts. The current sheet was thinning down to ∼3000 km during intervals *B* and *C*. Ion moments computed from HIA (C3) and CODIF (C1 and C4) ion distributions are very similar. The increases of the convective electric field $\mathbf{E}_c=-\mathbf{V}\times\mathbf{B}$ indicate a large rate of the magnetic flux transport during the three flow bursts. Thus, the criteria of the flow bursts ($|E_c|>$ 2 mV/m, e.g. Nakamura et al., 2001) are satisfied.

4 Detailed analysis of Cluster observations

In this section we analyze the magnetic field, ion moments and electron ET spectra during the three tailward flow intervals separately. We visually inspect the low-pass filtered (cut-off frequency is 1/8 Hz) 1-s averaged magnetic field time series and corresponding vector derivatives (magnetic field curl, magnetic tensions and magnetic pressure gradient) plotted in the GSM coordinate system to identify spatial

structures. Then, their properties are studied, using, if necessary, coordinate rotation.

4.1 Interval *A*

Figure 4 presents Cluster observations during the first tailward flow burst (03:40–03:47 UT, interval *A*). During the entire 7-min long interval Cluster was located in the northern half of the central plasma sheet. The magnetograms at all four spacecraft are of similar shape and close together. The most southern spacecraft (C3) showed the lowest B_x until ~03:45 UT. After 03:45 UT B_x at all four probes dropped to very low values, indicating an entrance to the thick sheet with uniformly weak magnetic field. The electric current density ($\mathbf{j}=\mu_0^{-1}\nabla\times\mathbf{B}$) varied between −4 and 4 nA/m^2, with $j_x>0$ and a set of bipolar variation of j_x and j_z till ~03:45 UT. Intervals of the two distinct magnetic field variations (between 03:41:40–03:43:00 UT and between 03:43:00–03:46:00 UT) are marked by *A*1 and *A*2, respectively. During interval *A*1, the angle between **j** and **b** ($\widehat{\mathbf{b},\mathbf{j}}$) deviates from 90° first to 30° at 03:42 UT, then to 140°, then gradually turns to the direction perpendicular to **b**. During interval *A*2, $\widehat{\mathbf{b},\mathbf{j}}$ varies between 100° and 180°. Cluster started to detect a tailward bulk flow with $V_x<-50$ km/s at ~03:41 UT. The Y-component of the bulk velocity was negligible comparing with V_x. The flow decays at ~03:47 UT. Until 03:44:40 UT, the $\mathbf{j}\times\mathbf{B}$ force was mainly contributed by the magnetic pressure gradient (∇P_b), the magnetic tension force ($\mu_0^{-1}(\mathbf{B}\cdot\nabla)\mathbf{B}$) was a factor of 2 smaller than ∇P_b; the $\nabla_z P_b$-component was the largest one and positive at $B_x>0$. Both the ion pressure P_i and the sum of ion and magnetic pressure $P_t=nkT_i+B^2/2\mu_0$ gradually increased until ~03:42 UT. At ~03:42 UT the ion pressure dropped down, showing a broad minimum during 03:43:30–03:45:30 UT. The total pressure decreased after 03:42 UT too, then increased with a local maximum at ~03:43:30 UT. During 03:43:30–03:45:30 UT the total pressure was 15% larger than the ion pressure. The cross-tail (Y) and vertical (Z) components of the $-\mathbf{V}\times\mathbf{B}$ electric field showed a broad maximum with E_y~4 mV/m and a minimum with E_z~−5 mV/m between 03:43:30–03:45:30 UT. The magnetic field fluctuations, calculated from non-filtered FGM data as standard deviations of B within 12 s (3 spins) sliding windows increased simultaneously with the bulk flow, but do not exceed $0.3\langle B\rangle$ during intervals of significant flux transfer ($E_c>2$ mV/m).

Performing the deHoffmann-Teller analysis (HT analysis, Khrabrov and Sonnerup, 1998) to the the first interval of enhanced tailward flow (03:41:40–03:44:10 UT), we determined the HT-frame velocity V_{HT}=[−276.7, −31.89, −78.52] (results for C1). The $\mathbf{E}_c$ vs. $\mathbf{E}_{HT}=\mathbf{V}_{HT}\times\mathbf{B}$ correlation coefficient is cc=0.98, and the linear regression slope is s=1.017 for C1. Results for C3 and C4 are very similar. Thus, the HT-frame is well determined, showing the presence of quasi-static structure moving mainly tailward in respect to the spacecraft. Regression analysis of the local Alfvén velocity $\mathbf{V}_a=\mathbf{B}/\sqrt{\rho\mu_0}$ and the ion velocity in the HT-frame $\mathbf{V}'=\mathbf{V}-\mathbf{V}_{HT}$ (Walén test) gives the correlation coefficient 0.15, and the slope 0.27 (see for comparison Eriksson et al., 2004). Thus, no significant plasma acceleration in the HT frame, required by the fast reconnection model, was detected.

The electron pitch-angle ET spectrograms from the PEACE instrument at all four spacecraft are shown in Fig. 5. The plot shows electron fluxes at energies in the range 50–10 000 eV, subdivided into 6 bins. The central energy for each bin is shown at the left panel. Each panel shows the pitch-angle distribution (PAD) in the specified energy range with the parallel flux (0° PA) on the bottom and the anti-parallel (180° PA) on the top of the panel. During interval *A*1 Cluster detected a low energy (~100–300 eV) electron flux parallel and anti-parallel to the magnetic field (0 and 180° more visible at C1, C2 and C4, and less visible at C3), and more isotropic at E ~1–3 keV. During interval *A*2 the low energy electron flux disappeared; Cluster detected an increasing flux of 0.5–3 keV 0 and 180° PA electrons. This flux increased is more pronounced at the most southern spacecraft C3, less pronounced at C1, C2, and C4. C2 started to detect the enhanced electron flux somewhat earlier than the other probes. Since the average magnetic field direction during the electron flux enhancement was [0.78, −0.56, −0.20] at C1, [0.61, −0.68, −0.38] at C2, [0.57, −0.66, −0.47] at C3, and [0.79, −0.54, −0.21] at C4, the ~1 keV electrons showed significant counter-streaming motion in the cross-tail ($\pm Y$) direction.

During interval *A*1 all four spacecraft detected significant and similar shape variations of the Y and Z magnetic field components, while amplitudes of B_x variations did not exceed ~5 nT. B_y at the barycenter, previously slightly negative, first increasee to 4 nT then decreased down to −9 nT, then increases again to 4 nT. B_z first increased up to 5 nT then decreased down to −2 nT.

Minimum Variance Analysis (MVA, e.g. Sonnerup and Scheible, 1998) of the magnetic field at the Cluster barycenter (average magnetic field at the four probes) yields for interval *A*1 the eigenvalues λ=[10.7, 3.32, 0.39], and the corresponding eigenvectors (in GSM) $\mathbf{N}_1$=[0.28, 0.91, 0.32], $\mathbf{N}_2$=[0.38, 0.19, −0.91], $\mathbf{N}_3$=[−0.88, 0.38, −0.29]. Thus, the maximum, intermediate and minimum variance component of the magnetic field are directed mainly along Y, $-Z$, and $-X$, respectively. Figure 6 shows the magnetic field time series during interval *A*1 in the MVA frame. The minimum and intermediate variance component variations have small amplitude, while the maximum variance component experiences two bipolar variations with amplitude of 15 nT. The traces of $B_{\max}$ are of the same shape at all four spacecraft, indicating a spatial structure passing by the Cluster constellation at the onset of the fast tailward flow. Figure 7 (panels a and b) presents the magnetic field vectors at the four spacecraft plotted in projection onto the XY (close to min–max) and XZ (close to min–int) planes. During interval *A*1, Cluster crosses a region where the magnetic field turns dawnward

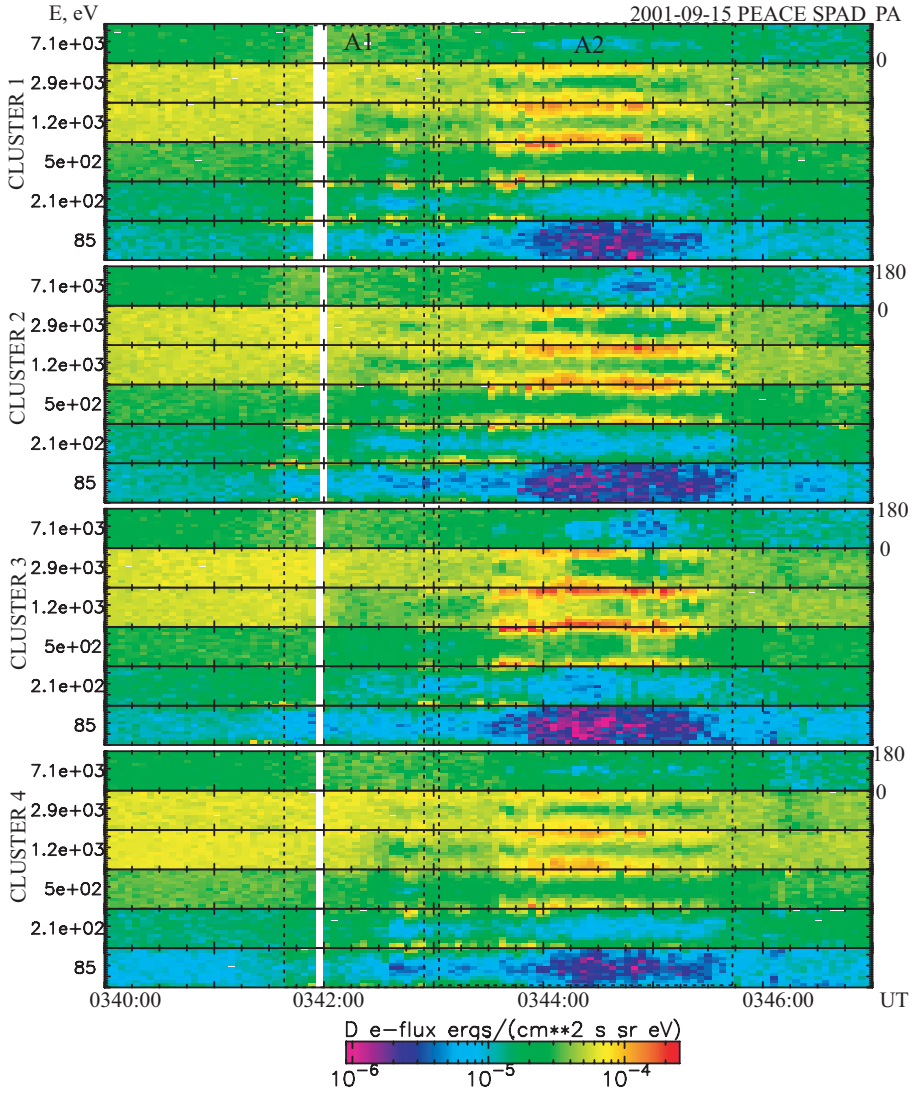

Fig. 5. Cluster PEACE pitch angle distribution (Spin PAD) energy-time spectrograms, interval A. Dashed line boxes show intervals *A*1 and *A*2.

and exhibits the bipolar north-to-south variation. C1, C2, and C3 showed a short increase of $|B|$, while C4 showed a local minimum of $|B|$.

The similarity of the $B_{\max}$ trace shapes at the four probes enables timing analysis (Harvey, 1998) of the $B_{\max}$. Four-point timing gives a unique solution of linear system for three components of the velocity normal to the planar boundary crossed by spacecraft. In our case, the dominant component of the plasma velocity is tailward (Fig. 4). We assume that the magnetic structure is transported by the plasma flow, i.e. moves tailward. Thus, a deviation of the timing normal from pure tailward direction gives a tilt of the boundary in XY and XZ planes, indicating a curved shape of the tailward moving magnetic structure encountered by the spacecraft constellation. Timing results are $\mathbf{V}_n$=[−0.35, −0.09, 0.93]·110 km/s for the first boundary (around the time mark 40 s) and $\mathbf{V}_n$=[−0.49, 0.66, −0.56]·160 km/s for the second one (time mark 60 s). An interpretation sketch is shown in Fig. 7c. The first boundary is moving tailward and northward, indicating Cluster encounters the tailward moving surge with the magnetic field elevation. The second one moves tailward and southward, indicating Cluster exit the magnetic surge. The Y-component of the normal to the first boundary is negative, however small, while for the second boundary, n_y is positive and large. These results may be interpreted as signatures of crossing the tailward moving magnetic structure with an ellipsoid-like boundary. The spacecraft crosses the structure close to its dawn-side edge, entering through dawnward moving boundary and exiting through duskward moving one. This boundary is shown by dashed line on the interpretation sketch (Fig. 7c). The presence of the north-south B_z variation and strong $-B_y$ may

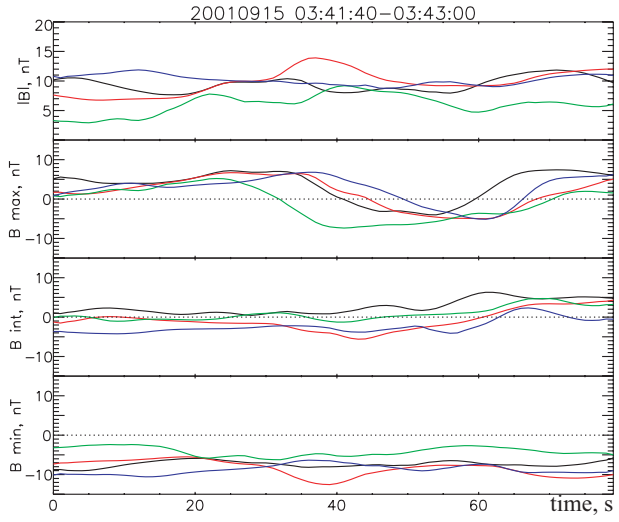

Fig. 6. Interval *A*1: Magnetic field observations in the variance frame. Time is in seconds after 03:41:40 UT.

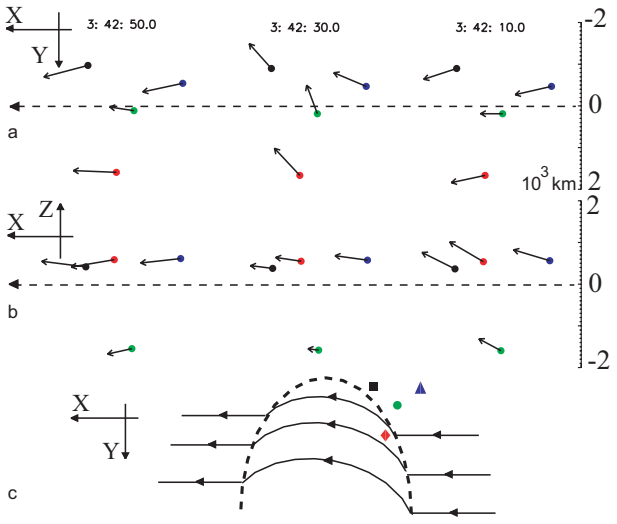

Fig. 7. Interval *A*1: Projections of the magnetic field at the four s/c (black arrows) onto the XY **(a)** and XZ **(b)** GSM planes at three successive instances. The 3-D interpretation cartoon **(c)** shows a view to the equatorial plane from above. The dashed arrow indicates the spacecraft barycenter motion relative to the magnetic structure. Thick dashed line denotes the boundary of the magnetic structure. The solid lines represent the magnetic field force lines.

be interpreted as signatures of the left-handed flux rope like structure (Slavin et al., 2003). Yet, the MVA results disagree with classic constant-α model (see, e.g. Slavin et al., 2003; Henderson et al., 2006). Since the spacecraft crossed an upper (northern) part of this structure only, we can not state that it is closed, forming a magnetic island. It also may be an NFTE-type (Sergeev et al., 1992) or CD-related (Ohtani et al., 2004) surge of the current sheet. The electric current deviated from the perpendicular direction to ∼150°, and $|\mathbf{j}\times\mathbf{B}|$ has a local minimum during *A*1. The *X*-aligned scale of this structure, estimated from the average V_x during 03:42:00–03:42:50 (∼170 km/s) and the duration of the structure observation, is ∼8000 km ∼1.25 R_E.

During interval *A*2 the total magnetic field first increased up to 15 nT, varies at this level, and decreased down to 1 nT. Since B_x is rather stable during the major part of this interval, except for the the drop at ∼03:45:30 UT, the increased of $|B|$ is due to large $|B_y|$ and $|B_z|$ (both are negative). Timing analysis of the $|B|$-traces (Fig. 4) gives for the first boundary (03:43:15–03:43:32 UT) $\mathbf{V}_n$=[−0.59, −0.41, −0.69]·194 km/s and for the second one (∼03:45:30 UT) $\mathbf{V}_n$=[−0.34, 0.76, 0.55]·101 km/s. Thus, show that the first boundary moved tailward, dawnward and southward while the second one moved tailward, duskward and northward. In a volume, bounded by these fronts, the magnetic field rotated from the Earthward-duskward-northward to Earthward-dawnward-southward enhancing its strength due to increase of cross-tail component magnitude, anti-parallel to the electric current. During a short time between ∼03:43:15–03:43:30 the magnetic tension and the magnetic pressure gradient were comparable and the Z-component of the magnetic tension force is negative (Cluster was in northern half of the plasma sheet). Then, the $\mathbf{j}\times\mathbf{B}$ force was dominated by the magnetic pressure gradient, and the Z-component of *B*-tension changes its sign to positive. Since $\nabla_z P_b$ dominates and $j_y>0$ and relatively stable, the spacecraft probe a sheet-like structure with the normal close to $Z_{\rm GSM}$.

Figure 8 presents the magnetic field vectors at the four spacecraft in XY- and XZ-planes at 03:43:00 UT (ahead of the structure), 03:44:00, 04:45:00 and 03:45:30 UT. The bottom panel presents an interpretation scheme: the solid lines present the magnetic filed field force lines. Cluster crossed an *X*-elongated magnetic field surge with the field-line curvature first directed along $-Z$ then along $+Z$. The structure was bounded in the cross-tail direction, and Cluster enters through its dawn-side boundary and crossed this object near its dawn-side edge (see Fig. 7c). This explains the fact, that most duskward probe (C2) started to detects the electron flux enhancement earlier and detected it longer than the others (see Fig. 5). The duration of this structure is about 130 s and average ion velocity ∼315 km/s, which gives the structure length ∼6 R_E. These observations may be interpreted as the signatures of the post plasmoid plasma sheet (e.g. Ieda et al., 1998) with an *X*-elongated southward magnetic field loop.

4.2 Interval *B*

Figure 9 presents the Cluster measurements and the magnetic field derivatives calculated during interval *B*. A magnetic field structure, associated with the E_c enhancement up to ∼4 mV/m, was observed between 03:49:30–03:50:30 UT (dashed-line box). The tailward velocity grows up to $|V|$∼400 km/s. The magnetic field absolute value

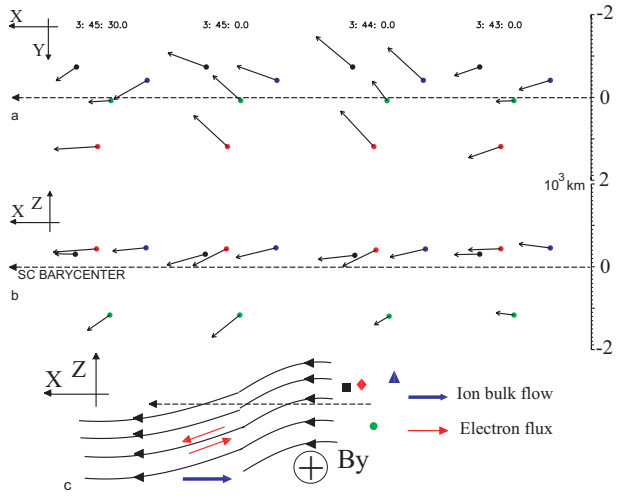

Fig. 8. Interval *A*2: Projections of the magnetic field at the four s/c (black arrows) on *XY* **(a)** and on *XZ* **(b)** GSM planes at four successive instances. Panel **(c)** presents the interpretation cartoon.

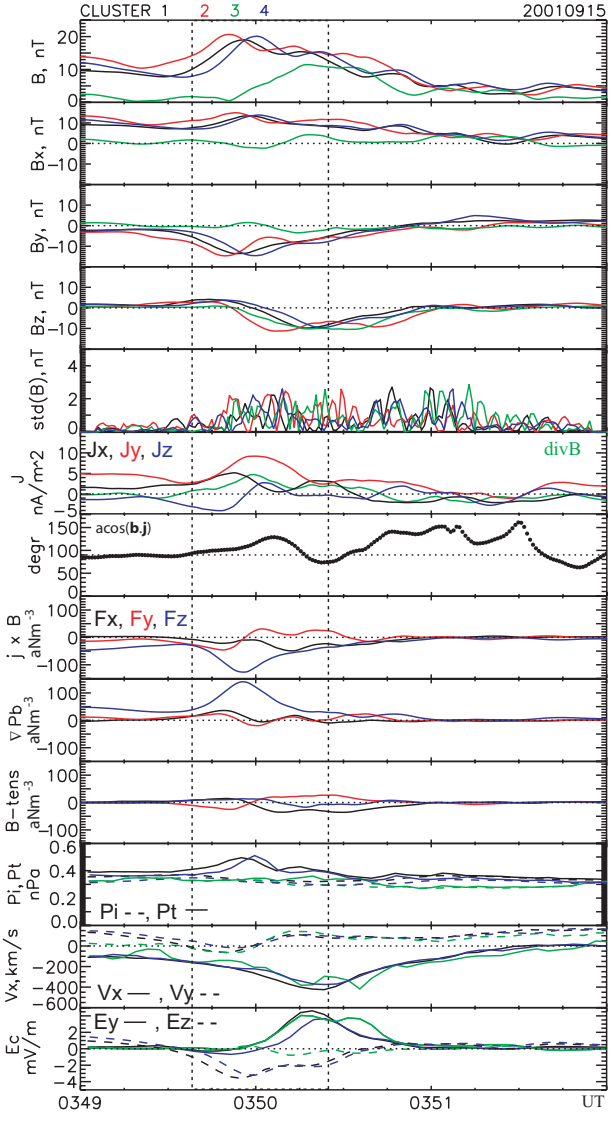

Fig. 9. Cluster observation during interval *B*: The same format as in Fig. 4.

increased from ∼10 to ∼20 nT. B_x is positive at C1, C2 and C4 (the northern group), while the most southern probe (C3) measured B_x fluctuating near zero level. B_x at the northern group increased around 03:50:00 UT, while B_x at C3 slightly decreased, down to −4 nT at this time. B_y shows a remarkable north-south difference: B_y at the northern group displayed a pronounced minimum with the value of −17 nT around 03:50:00 UT (∼15 s early at C2), while B_y at C3 slowly varied around zero with a local maximum (∼2 nT) at this instance. B_z at the northern group exhibited a clear bipolar variation, changing from ∼4 to ∼−10 nT. B_z at C3 showed no positive variation, gradually decreasing from approximately zero to ∼−10 nT. The Y-component of the current density was positive, while j_x and j_z ($j_y > |j_x|, |j_z|$) showed bipolar variations (j_z changes sign from negative to positive). **j** was close to be perpendicular to the magnetic field ahead of the structure; **b**, **j** varied between 90° and 120° inside the structure, because of the duskward rotation of **b** with ∇B directed mainly northward (**j** deviation from the nominal direction did not exceed 20° around 03:50:00 UT). The Z-component of the $\mathbf{j}\times\mathbf{B}$ force was negative ($B_x > 0$ at the Cluster barycenter; $|(\mathbf{j}\times\mathbf{B})_z| > |(\mathbf{j}\times\mathbf{B})_x|, |(\mathbf{j}\times\mathbf{B})_y|$). The magnetic field gradient was a factor of 7 larger than the B-tension force. The major contribution to the force was from $\nabla_z P_b$. The X-component of the B-tension force changed sign from positive to negative, corresponding to the B_z change. The Y- and Z-components of the B-tension force were approximately of the same value as the X-component, and changed their signs from negative to positive (Y) and from positive to negative (Z), indicating that Cluster crossed a 3-D structure. The total pressure at C1 and C4 had a local maximum near 03:49:45 UT, while P_t at C3 shows no significant change. The ion thermal pressure slightly decreased. Both B_y and B_z turned back to nearly zero after the structure passage.

HT analysis of the the C4 data during interval *B* gives $\mathbf{V}_{HT}$=[−323.2, 104.2, −26.86], the HT-frame is well defined: cc=0.99 and the s=1.034. Walén test with cc=0.66 and s=0.319 shows no significant plasma acceleration in the HT-frame. The local Alfvén velocity was ∼400 km/s.

The electron ET spectra for interval *B* are shown in Fig. 10. The enhancement of parallel and anti-parallel electron flux in the energy range of 0.5–3 keV was detected between 03:50:00–03:50:45 UT. C2, again, started to detect the electron flux enhancement earlier and detected it during longer time than the other probes. The flux of electrons with energies <300 eV sufficiently decreases. The average magnetic field direction during the electron flux enhancement

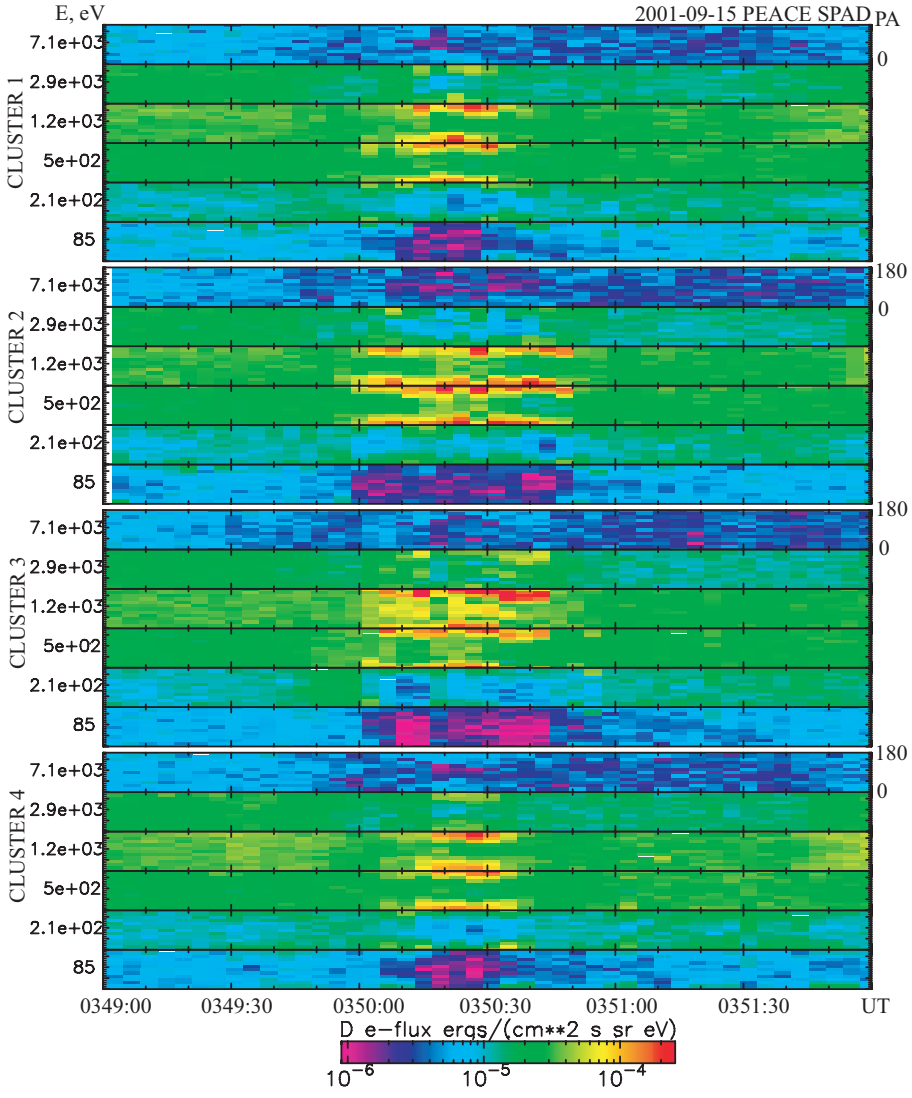

Fig. 10. Cluster PEACE PAD ET spectrograms, interval *B*.

was [0.75, −0.39, −0.45] at C1, [0.68, −0.37, −0.61] at C2, [0.11, −0.18, −0.95] at C3, and [0.71, −0.48, −0.42] at C4. The parallel and anti-parallel electron fluxes started increasing about 10 s later on the center of the magnetic structure (B_z=0) was detected.

The magnetic field variations (increase of $|B|$, strong B_y<0, north-to-south variation of B_z), observed by the northern group of the spacecraft (C1, C2, and C4) may be interpreted as the signatures of a left-handed flux rope (Slavin et al., 2003). Staying near B_x=0, C3, however, showed different signatures: $B_y \geq 0$, B_z<0 (no bipolar signatures), no increase of P_b. According to the flux rope interpretation, one expects the same direction of the core filed in the center and at the northern half of the rope. The proper interpretation should explain the B_y difference, and the absence of bipolar signatures in C3 *B*-trace.

Since the average direction of the current density vector was close to *Y* ($\mathbf{e}_j$=[0.37, 0.80, −0.19]) and the average direction of the magnetic pressure gradient, pointing along the normal, was close to *Z* ($\mathbf{e}_{pb}$=[0.22, 0.10, 0.94]), the GSM system is a good proxy for the natural coordinates. Figure 11a–c presents a multi-point view of the magnetic field structure in *XY*, *XZ*, and *YZ* planes. The observations are interpreted in the following way. During 03:49:30–03:50:30 UT Cluster crossed a magnetic loop, closed from the tailward side with the north-south size comparable or larger than the Cluster inter-spacecraft separation, embedded into a more thicker current sheet C3, crossing the the structure near it's axis did not detect a northward B_z, showing B_z<0, while the northern group (C1, C2, C4) detected north to south B_z variation. The northward B_z turn is due to local magnetic field compression by the plasma flow. This can

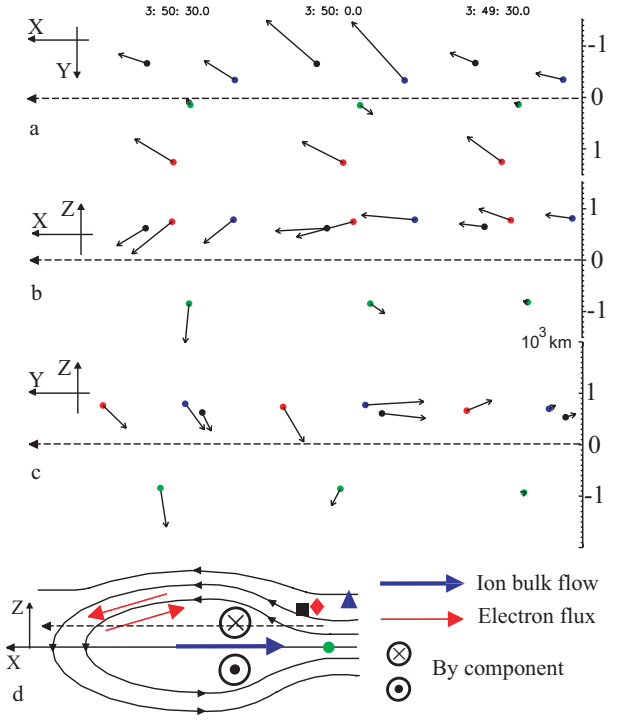

Fig. 11. Interval B: Projections of the magnetic field at the four s/c (black arrows) onto XY **(a)**, XZ **(b)**, and YZ **(c)** GSM planes at three successive instances. Panels d presents the interpretation cartoon.

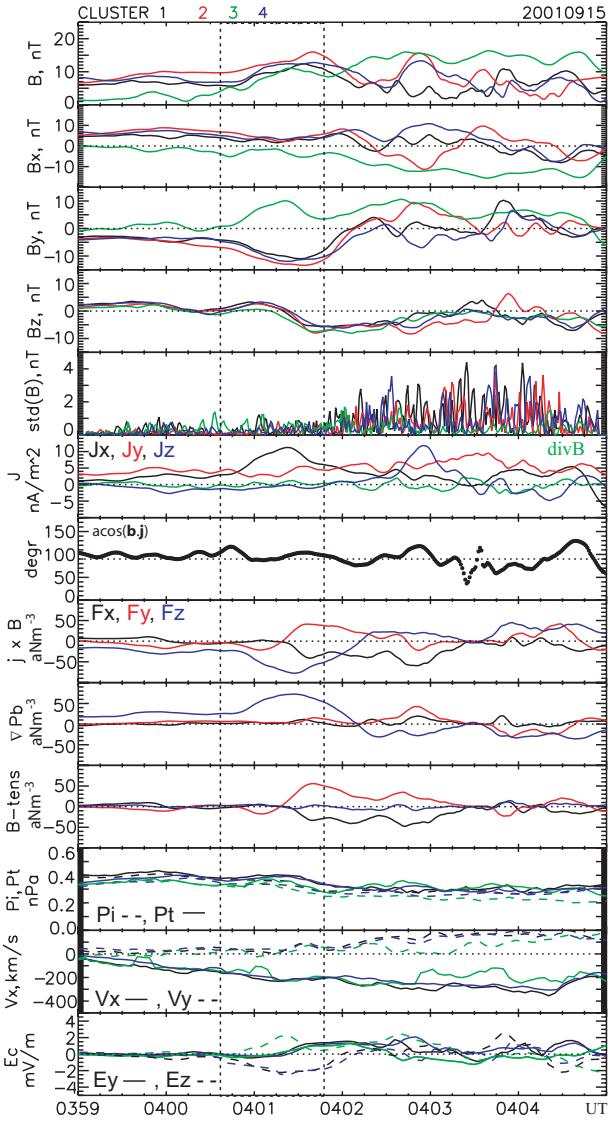

Fig. 12. Cluster observation during interval C: The same format as in Fig. 4.

explain the increase of the magnetic pressure, detected by the northern group. Thus, the situation resembling rather NFTE with the magnetic structure similar to quasi-plasmoid configuration obtained in simulations of nonlinear plasmoid evolution (Abe and Hoshino, 2001), than a flux rope. However, the observed structure is more complex, including an out-of-plane magnetic field component (B_y) directed dawnward in the northern half and, likely, duskward in the southern half of the loop (C3 at $B_x \leq 0$ detects $B_y \geq 0$). The length of this structure along X-direction, estimated using $\langle V_x \rangle \sim 150$ km/s and the structure duration, ~ 60 s, is $\sim 1.5\, R_E$.

The magnetic field variation as well as the electron flux enhancement was first detected by C2, then by C3, C1 and finally by C4. This indicates that the magnetic structure was bounded in cross-tail direction, and crossed by Cluster near its dawn-side boundary, like it shown in Fig. 7c (valid for northern half of the structure only). In this case, C2 stayed within the structure longer than than the other probes, which can explain a longer interval of enhanced electron flux, observed by C2. The enhancement of bi-directional electron flux indicates, that the loop is closed further downtail.

4.3 Interval *C*

Figure 12 presents summary plot of Cluster measurements during interval C, when Cluster detects the tailward ion flow with maximum velocity of 400 km/s. Magnetic field variations, associated with significant flux transfer ($E_c \sim 3$ mV/m, $|E_{cz}| > E_{cy}$) were detected during 04:00:30–04:02:00 UT (dashed-line box). The magnetic field absolute value increased from ~ 5 to ~ 15 nT while B_x decreases. B_y at C1, C2, and C4 (all are situated in the northern part of the plasma sheet) experienced a negative variation with amplitude of 10 nT, while B_y at C3, located near the neutral sheet in the southern part of the sheet ($-5 < B_x < -1$ nT), exhibited a positive B_y variation with amplitude of 10 nT. All four probes detected bipolar variation of B_z with $B_z \sim 0$ at the maximum of $|B_y|$. These magnetic field variations corresponded to a local enhancement of the X-component of the current density. The $\mathbf{j} \times \mathbf{B}$ force had a local maximum in Z- and a bipolar variation in the Y-components. $[\mathbf{j} \times \mathbf{B}]_x$ stayed close to zero until

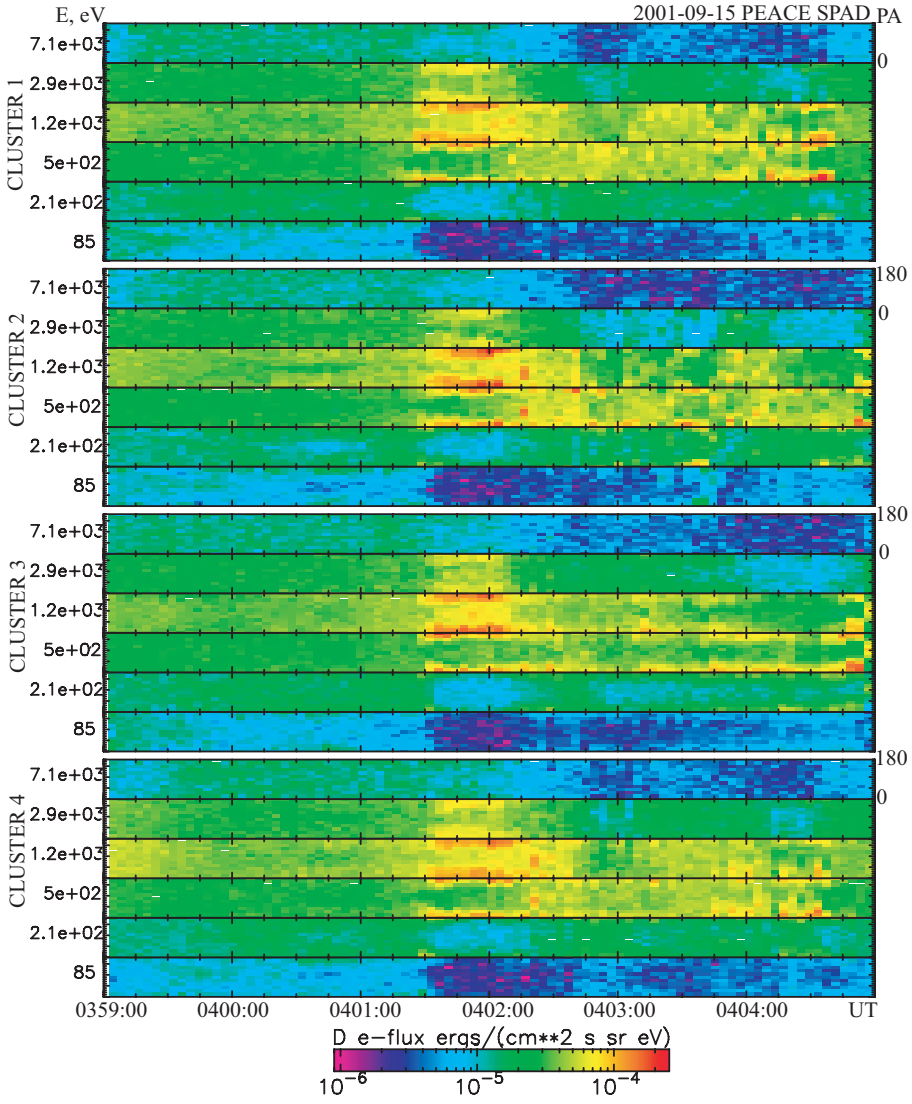

Fig. 13. Cluster PEACE PAD energy-time spectrograms, interval *C*.

∼04:01:20 UT then turned negative simultaneously with the decrease of the total and ion pressures. The center of the bipolar B_z variation coincided with the local maximum of P_t. The current density vector was directed mainly perpendicular to the instantaneous magnetic field: ($(\widehat{\mathbf{bj}})$ varied between 80–120°).

HT analysis of the C1 data during 03:59:40–04:02:00 UT results with $\mathbf{V}_{HT}$=[−208.7, 56.14, −57.86] km/s with well defined HT-frame: cc=0.98, s=1.01. Walèn test with cc=0.511 and s=0.226 again shows vanishing acceleration of plasma in the HT-frame.

Figure 13 presents electron ET spectrograms for interval *C*. During 04:01:30–04:02:30 UT, when the above described magnetic field structure was observed, all the four spacecraft detected local enhancement of parallel and antiparallel electron fluxes with energies of 0.5–3 keV. The flux enhancement was first detected by C1 and C3, then by C2 and C4, contrary to the observations during interval *B*. Some, but smaller enhancement of the perpendicular flux was also detected mainly after 04:02:00 UT. Again a sufficient decrease of low energy <200 eV electron flux after 04:01:30 UT was detected. The average magnetic field direction during the electron flux increase was [0.21, −0.19, −0.64] at C1, [0.34, −0.27, −0.59] at C2, [−0.52, 0.51, −0.66] at C3, and [0.53, −0.49, −0.53] at C4. The electron flux features were the same at C3, situated in the southern half of plasma sheet detecting duskward magnetic field, and at C1, C2, C4, located in the northern half and detecting dawnward magnetic field. The increase of electron flux started about 10–15 s later than B_z=0 was detected (∼04:01:15 UT).

Although the B_y and B_z signatures during 04:01:00–04:02:00 UT were similar to that during interval *B*, the B_x

behavior, and timing of the bi-polar B_z variations at the four probes are different. The difference between B_x at the northern group and that at C3 (ΔB_x) decreased while ΔB_y increased, indicating a presence of X-directed current. Figure 14 shows projections of the magnetic field vectors at the four spacecraft onto XY, XZ, and YZ planes at 04:01:00 and 04:01:30 UT. At 04:01:00 UT Cluster crossed the loop with northward directed magnetic field ($B_z>0$), and at 04:01:30 UT Cluster crosses the loop of southward directed magnetic field ($B_z<0$). Timing of B_z time series shows that the maximum B_z was first detected by C1 then by C3, C2, and, finally, by C4. The lag time vector (with respect to C1) is dt=[6., 5., 8.] s, which gives the normal velocity $\mathbf{V}_n$=[−0.91, 0.42, 0.04]·210 km/s. The minimum B_z was detected with the lag dt=[6, 4, 10] s with respect to C1. This gives $\mathbf{V}_n$=[−0.93, 0.28, 0.23]·170 km/s: contrary to observations during interval B, the both boundaries move duskward with respect to the spacecraft. The magnetic field observations showed signatures of a current filament, with $j_x>j_y$, transported by the ion bulk flow. Cluster crossed the magnetic structure entering through its dusk-side boundary with $(\mathbf{B}\cdot\nabla)\mathbf{B}<0$, and exiting through its dawn-side boundary, detecting $(\mathbf{B}\cdot\nabla)\mathbf{B}>0$. The interpretation scheme is shown in Fig. 14d and e. Although the magnetic tension magnitude is comparable with that of the magnetic pressure gradient, the structure was not force-free, because the B-tension force was directed mainly along $\pm Y$, while the ∇P_b was directed mainly along Z. Current density vector did not significantly deviate from the B-perpendicular direction. The cross-tail size of this structure may be roughly estimated using mean value of V_y at 04:01:00–04:01:45 UT, equals to ∼60 km/s and the lag between negative and positive $(\mathbf{B}\cdot\nabla)\mathbf{B}$ peaks, ∼45 s. This yields L_y=2700 km∼0.5 R_E. The scale along X estimated form $\langle V_x\rangle$∼200 km/s and the structure duration is about 1.5 R_E.

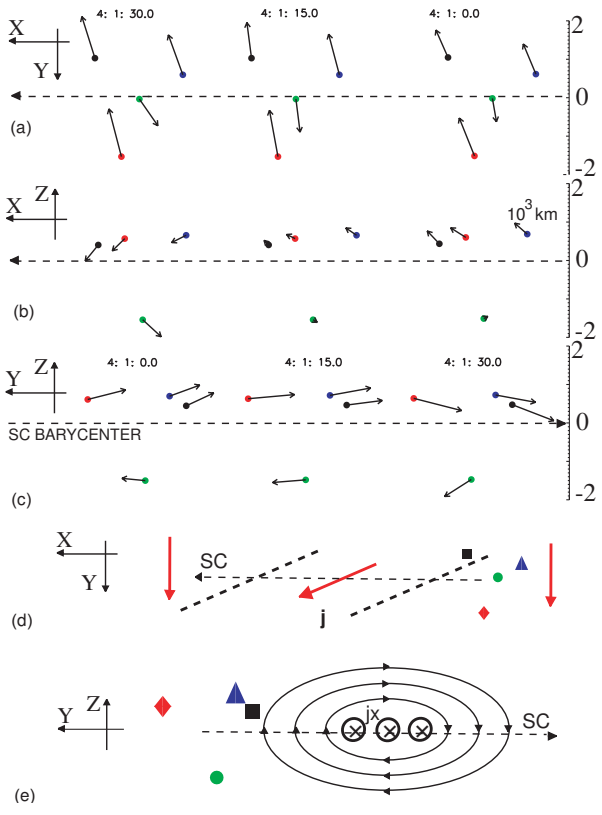

Fig. 14. Interval C: Projections of the magnetic field at the four s/c (black arrows) onto XY **(a)**, XZ **(b)**, and YZ GSM planes at the three successive instances. Note, that time increases from right to left in panels (a) and (b), and from left to right in panel **(c)**, according to the spacecraft pass (dashed arrow) through the structure. Panels **(d)** and **(e)** present the interpretation scheme. Red arrows in panel (d) indicate the electric current direction.

5 Discussion and conclusions

We have shown in-situ observations of three successive 2–7 min long tailward flow bursts with velocities of about 400 km/s detected in the near-Earth magnetotail at $X_{\rm GSM}$=−18.9 R_E near the midnight meridian. In contrast with previously discussed observations of tailward fast flows in the near-Earth magnetotail (Nagai et al., 1998a; Eriksson et al., 2004; Miyashita et al., 2005), these three flow bursts were observed during northward IMF. IMF B_z was northward (of 5–10 nT) during ∼2.5 h before the first tailward flow was observed. IMF B_y was mainly dawnward and fluctuating. The first flow was detected 2.5 h after the large substorm followed by B_z decreasing after a strong dipolarization (see Fig. 1), accompanied by the gradual increase of the magnetic gradient in the current sheet. Thus, the activity in the near-Earth magnetotail plasma sheet, leading to tailward flows, was, likely, internally triggered.

The magnetic field fluctuations $\sigma(B)$ were about $0.4\langle B\rangle$ during the flow bursts, therefore turbulent current disruption, implies $\sigma(B)\sim\langle B\rangle$ (e.g. Lui, 1996; Lui et al., 2006), hardly can be a mechanism of the flow generation. j_y is positive and increases during the flow intervals B and C, thus, the ballooning mechanism, implying the generation of the dusk-dawn component of the electric current (Roux et al., 1991, 2006), can not be considered as the source of these two tailward flow bursts either. During interval A, however, j_y was oscillating between −1 to 3 nA/m^2 with a peak-to-peak period ∼30 s. This may be interpreted as the quasi-periodic generation of the dusk-dawn current. We also found the systematic lag between the magnetic field fluctuations at C1 and C2 (separated mainly along Y), indicating azimuthal propagating waves, predicted by the models of CD (Roux et al., 1991; Lui, 1996). No signatures of fast reconnection (see, e.g. Semenov et al., 2004) were found during the three flow bursts: Plasma velocity in the de Hoffmann-Teller frame did not exceed 25% of the Alfvèn speed, which is much smaller than the acceleration, predicted by fast reconnection model

(see, e.g. Eriksson et al., 2004). Thus, the tailward flows were generated rather due to a weak reconnection on closed field lines (or in the course of X-line formation by the ballooning type perturbation).

The three flow bursts were associated with a local auroral activation in the MLT sector of the Cluster foot point, ∼5° equatorward. The time relationship between plasmoids and auroral pseudo-breakups was studied by Ieda et al. (2001). They found that the earliest plasmoid was observed at X=−28 R_E about 2 min before the auroral brightening. Typically, plasmoids are observed 0–2 min after the brightening. This was interpreted that reconnection occurs before the auroral activation, and a "young" plasmoid is observed before or simultaneously with the brightening if the spacecraft is located near the reconnection site. It follows from this model, that during intervals *A* and may be *C* Cluster was situated near the reconnection site, while during interval *B* reconnection occurs closer to the Earth. It should be noted, however, that this interpretation is based on a 2-D model with a plasmoid infinity long in cross-tail direction. Our observations show that the magnetic structures, observed during tailward flows in the near-Earth tail, are localized in the Y_{GSM} direction. Nakamura et al. (2001) studied the relative timing between the bulk flow bursts (mainly Earthward), observed in the near tail, and localized auroral activations. They found that on average, the aurora precedes the flow activations by 0–3 min. If the auroral activations starts within 1 h MLT difference and 2° latitude distance from the spacecraft foot point, the time delay is reduced down to less than 30 s. Our results for the tailward flows are similar: The auroral activation during intervals *A*, with the minimum delay with respect to the maximum $|E_c|$ observation, was observed around the MLT of the Cluster foot point; delays for *B* and *C* activations, observed within ±0.5 h MLT, are of −2.5 and +3 min, respectively.

Each observed flow burst corresponds to a similar magnetic field variations. The magnetic field turns dawnward (duskward) in the northern (southern) half of the plasma sheet. The spacecraft, situated above the neutral sheet detected a more or less pronounced north-to-south bipolar variations of the magnetic field. All probes show the southward magnetic field around minima of the flow velocity. The magnetic field magnitude increases by ∼10 nT, and this increase is due to an enhancement of B_y. A total pressure enhancement, considered as the signature of a plasmoid (Ieda et al., 1998), was observed during the interval *B* only, when the ion pressure was nearly constant. The increase of the magnetic pressure was compensated by a decrease of the ion pressure during intervals *A* and *C*.

The important and novel aspect of this case study is that, contrary to the case studies with small spacecraft tetrahedron (e.g. Eastwood et al., 2005; Henderson et al., 2006), the spacecraft configuration gives the possibility to monitor the neutral sheet vicinity $B_x \approx 0$ and the plasma sheet at $B_x \approx$10–15 nT simultaneously, allowing to distinguish between a closed plasmoid-like magnetic field configuration and an NFTE-like one, with a tailward-open magnetic surge. The analysis of the four-point magnetic field measurements have shown that the aforementioned bipolar north-to-south magnetic field variations, commonly interpreted as signatures of plasmoid or flux ropes, are not necessarily indications of a closed O-type magnetic field structure. They may be signatures of the NFTE-like surge (interval *B*) or indicate a crossing of an Earthward-duskward directed current filament (interval *C*).

In contrast to results, reported by Zong et al. (2004), the bi-directional electron fluxes were detected after the bipolar variation detections. They associated, therefore, with the NFTE-like southward magnetic field loops, indicating that they are closed further in tail. The spacecraft enters into the flux tubes, containing the bi-directional electron flux, after crossing the flow boundaries, manifesting as the bi-polar magnetic field variations.

The B_y signs in these cases are different in the northern and southern halves of the plasma sheet. Thus this is neither a core field, assumed to be the same direction in both halves in the flux rope models, nor the guide field enhanced due to pile-up effect in localized reconnection of sheared magnetic field with a finite cross-tail length of *X*-line (Shirataka et al., 2006), but corresponds rather to the quadrupolar magnetic structure due to the Hall effect near X-line (Nagai et al., 1998b), It was shown, that the Hall currents, existing in the ion diffusion region, are closed by the system of the field-aligned currents (FAC), which may exist far away from the X-line, keeping the cross-tail magnetic field component, negative in the northern and positive in the southern halves of the sheet (e.g. Fujimoto et al., 2001; Treumann et al., 2006). This cross-tail field, originated by the Hall currents, may be enhanced by the magnetic field compression within fast flow bursts. The tailward moving filament of the Earthward-duskward directed current crossed by Cluster during interval *C* (see Fig. 14) may also be a part of the FAC system, related to the Hall currents in the reconnection region, localized in the cross-tail direction.

The important outcome of this work is the reconstruction of 3-D shapes of the magnetic structures, embedded into the tailward plasma flows. Using the spacecraft separation in the cross-tail direction, we found that the NFTE-like surges (intervals *A* and *B*) have ellipsoidal shapes. The spacecraft cross their dawn-side boundaries.

Acknowledgements. We thank H.-U. Eichelberger, G. Laky, C. Mouikis, L. Kistler, E. Georgescu and E. Penou for help with data and software, M. Hoshino, V. A. Sergeev, C. J. Owen and V. S. Semenov for valuable suggestions. This work was fruitfully discussed by ISSI team 91. We acknowledge NASA/GSFC, CDAWeb, DARTS/Geotail, and WDC for Geomagnetism data providers. We thank H. Singer for providing high resolution GOES 8 data. The CANOPUS and NORDSTAR arrays are funded by Canadian Space Agency. The IMAGE FUV investigations were supported by NASA through SWRI subcontract. The work by M. Volwerk was finan-

cially supported by the German Bundesministerium für Bildung und Forschung and the Zentrum für Luft- und Raumfahrt under contracts 50 OC 0104.

Topical Editor I. A. Daglis thanks two anonymous referees for their help in evaluating this paper.

References

Abe, S. A. and Hoshino, M.: Nonlinear evolution of plasmoid structure, Earth Planets Space, 53, 663–671, 2001.

Angelopoulos, V., Baumjohann, W., Kennel, C. F., Coroniti, F. V., Kivelson, M. G., Pellat, R., Walker, R. J., Lühr, H., and Paschmann, G.: Bursty bulk flows in the inner central plasma sheet, J. Geophys. Res., 97, 4027–4039, 1992.

Baker, D. N., Pulkkinen, T. I., Angelopoulos, V., Baumjohann, W., and McPherron, R. L.: Neutral line model of substorms: Past results and present view, J. Geophys. Res., 101, 12 975–13 010, 1996.

Balogh, A., Carr, C. M., Acuña, M. H., Dunlop, M. W., Beek, T. J., Brown, P., Fornacon, K.-H., Georgescu, E., Glassmeier, K.-H., Harris, J., Musmann, G., Oddy, T., and Schwingenschuh, K.: The Cluster magnetic field investigation: Overview of in-flight perfomance and initial results, Ann. Geophys., 19, 1207–1217, 2001, http://www.ann-geophys.net/19/1207/2001/.

Baumjohann, W., Paschmann, G., and Lühr, H.: Characteristics of high-speed flows in the plasma sheet, J. Geophys. Res., 95, 3801–3809, 1990.

Baumjohann, W., Hesse, M., Kokubun, S., Mukai, T., Nagai, T., and Petrukovich, A. A.: Substorm dipolarization and recovery, J. Geophys. Res., 104, 24 995–25 000, 1999.

Chanteur, G.: Spatial interpolation for four spacecraft: Theory, in: Analysis Methods for Multi-Spacecraft Data, edited by: Paschmann, G. and Daly, P., pp. 349–369, ESA, Noordwijk, 1998.

Eastwood, J. P., Sibeck, D. G., Slavin, J. A., Goldstein, M. L., Lavraud, B., Sitnov, M., Imber, S., Balogh, A., Lucek, E. A., and Dandouras, I.: Observations of multiple X-line structure in the Earth's magnetotail current sheet: A Cluster case study, Geophys. Res. Lett., 32, L11105, doi:10.1029/2005GL022509, 2005.

Eriksson, S., Öieroset, M., Baker, D. N., Mouikis, C., Vaivads, A., Dunlop, M. W., Rème, H., Ergun, R. E., and Balogh, A.: Walén and slow mode shock analyses in the near-Earth magnetotail in connection with a substorm onset on 27 August 2001, J. Geophys. Res., 109, A05212, doi:10.1029/2004JA010534, 2004.

Fujimoto, M., Nagai, T., Yokokawa, N., Yamade, Y., Mukai, T., Saito, Y., and Kokubun, S.: Tailward electrons at the lobe-plasma sheet interface detected upon dipolarizations, J. Geophys. Res., 106, 21 255–21 262, 2001.

Harris, E. G.: On a plasma sheet separating regions of oppositely directed magnetic field, Nuovo Cimento, 23, 115–121, 1962.

Harvey, C. C.: Spatial gradients and volumetric tensor, in: Analysis Methods for Multi-Spacecraft Data, edited by: Paschmann, G. and Daly, P., pp. 307–322, ESA, Noordwijk, 1998.

Henderson, P. D., Owen, C. J., Alexeev, I. V., Slavin, J., Fazakerley, A. N., Lucek, E., and Rème, H.: Cluster observations of flux rope structures in the near-tail, Ann. Geophys., 24, 651–666, 2006, http://www.ann-geophys.net/24/651/2006/.

Hesse, M., Birn, J., Kuznetsova, M. M., and Dreher, J.: A simple model of core field generation during plasmoid evolution, J. Geophys. Res., 101, 10 797–10 804, 1996.

Hones, E. W.: Transient phenomena in the magnetotail and their relation to substorms, Space Sci. Rev., 23, 393–410, 1979.

Hoshino, M., Mukai, T., Terasawa, T., and Shinohara, I.: Superthermal electron acceleration in magnetic reconnection, J. Geophys. Res., 106, 25 972–25 997, 2001.

Ieda, A., Machida, S., Mukai, T., Saito, Y., Yamamoto, T., Nishida, A., Terasawa, T., and Kokubun, S.: Statistical analysis of the plasmoid evolution with Geotail observations, J. Geophys. Res., 103, 4453–4466, 1998.

Ieda, A., Fairfield, D. H., Mukai, T., Saito, Y., Kokubun, S., Liou, K., Meng, C.-I., Parks, G. K., and Brittnacher, M. J.: Plasmoid ejection and auroral brightenings, J. Geophys. Res., 106, 3845–3857, 2001.

Johnstone, A. D., Alsop, C., Burge, S., Carter, P. J., Coates, A. J., Coker, A. J., Fazakerley, A. N., Grande, M., Gowen, R. A., Gurgiolo, C., Hancock, B. K., Narheim, B., Preece, A., Sheather, P. H., Winningham, J. D., and Woodliffe, R. D.: PEACE: A plasma electron and current experiment, Space Sci. Rev., 79, 351–398, 1997.

Khrabrov, A. V. and Sonnerup, B. U. Ö.: DeHoffmann-Teller analysis, in: Analysis Methods for Multi-Spacecraft Data, edited by: Paschmann, G. and Daly, P., pp. 221–248, ESA, Noordwijk, 1998.

Lui, A. T. Y.: Current disruption in the Earth's magnetosphere: Observations and models, J. Geophys. Res., 101, 13 067–13 088, 1996.

Lui, A. T. Y.: Potential plasma instabilities for substorm expansion onsets, Space Sci. Rev., 113, 127–206, 2004.

Lui, A. T. Y., Zheng, Y., Zhang, Y., Livi, S., Rème, H., Dunlop, M. W., Gustafsson, G., Mende, S. B., Mouikis, C., and Kistler, L. M.: Cluster observation of plasma flow reversal in the magnetotail during a substorm, Ann. Geophys., 24, 2005–2013, 2006, http://www.ann-geophys.net/24/2005/2006/.

Miyashita, Y., Ieda, A., Kamide, Y., Machida, S., Mukai, T., Saito, Y., Liou, K., Meng, C.-I., Parks, G. K., McEntire, R. W., Nishitani, N., Lester, M., Sofko, G. J., and Villain, J.-P.: Plasmoids observed in the near-Earth magnetotail at $X\sim-7\ R_E$, J. Geophys. Res., 110, A12214, doi:10.1029/2005JA011263, 2005.

Mukai, T., Fujimoto, M., Kokubun, S., Machida, S., Maezawa, K., Nishida, A., Saito, Y., Terasawa, T., and Yamamoto, T.: Structure and kinetic properties of plasmoids and their boundary regions, J. Geomag. Geoelectr., 48, 541–560, 1996.

Nagai, T., Fujimoto, M., Nakamura, R., Saito, Y., Mukai, T., Yamamoto, T., Nishida, A., Kokubun, S., Reeves, G. D., and Lepping, R. P.: Geotail observations of a fast tailward flow at X_{GSM}=-15R$_E$, J. Geophys. Res., 103, 23 543–23 550, 1998a.

Nagai, T., Fujimoto, M., Saito, Y., Machida, S., Terasawa, T., Nakamura, R., Yamamoto, T., Mukai, T., Nishida, A., and Kokubun, S.: Structure and dynamics of magnetic reconnection for substorm onsets with Geotail observations, J. Geophys. Res., 103, 4419–4440, 1998b.

Nagai, T., Nakamura, M. F. R., Baumjohann, W., Ieda, W., Shinohara, A., Machida, S., , Saito, Y., and Mukai, T.: Solar wind control of the radial distance of the magnetic reconnection site in the magnetotail, J. Geophys. Res., 110, A09208, doi: 10.1029/2005JA011207, 2005.

Nakamura, R., Baumjohann, W., Brittnacher, M., Sergeev, V. A., Kubyshkina, M., Mukai, T., and Liou, K.: Flow bursts and auro-

ral activations: Onset timing and foot point location, J. Geophys. Res., 106, 10 777–10 789, 2001.

Nakamura, R., Baumjohann, W., Mouikis, C., Kistler, L. M., Runov, A., Volwerk, M., Asano, Y., Vörös, Z., Zhang, T. L., Klecker, B., Rème, H., and Balogh, A.: Spatial scale of high-speed flows in the plasma sheet observed by Cluster, Geophys. Res. Lett., 31, L09894, doi:10.1029/2004GL019558, 2004.

Ohtani, S., Kokubun, S., and Russell, C. T.: Radial expansion of the tail current disruption during substorms: A new approach to the substorm onset region, J. Geophys. Res., 97, 3129–3136, 1992.

Ohtani, S. I., Shay, M. A., and Mukai, T.: Temporal structure of the fast convective flow in the plasma sheet: Comparison between observations and two-fluid simulations, J. Geophys. Res., 109, A03210, doi:10.1029/2003JA010002, 2004.

Øieroset, M., Phan, T. D., Lin, R. P., and Sonnerup, B. U. Ö.: Walén and variance analyses of high-speed flows observed by Wind in the midtail plasma sheet: Evidence for reconnection, J. Geophys. Res., 105, 25 247–25 264, 2000.

Paschmann, G., Papamastorakis, I., Sckopke, N., Haerendel, G., Sonnerup, B. U. Ø"., Bame, S. J., Asbridge, J. R., Gosling, J. T., Russel, C. T., and Elphic, R. C.: Plasma acceleration at the Earth's magnetopause: Evidence for reconnection, Nature, 282, 243–246, 1979.

Paschmann, G., Baumjohann, W., Sckopke, N., Papamastorakis, I., and Carlson, C. W.: The magnetopause for large magnetic shear – AMPTE/IRM observations, J. Geophys. Res., 91, 11 099–11 115, 1986.

Petschek, H. E.: Magnetic field annihilation, in: AAS/NASA Symposium on the Physics of Solar Flares SP-50, edited by: Ness, W. N., pp. 425–439, NASA, Washington, D.C., 1964.

Rème, H., Aoustin, C., Bosqued, J. M., Dandouras, I., Lavraud, B., Sauvaud, J.-A., Barthe, A., Bouyssou, J., Camus, T., Coeur-Joly, O., et al.: First multispacecraft ion measurements in and near the Earth's magnetosphere with the identical Cluster ion spectrometry (CIS) experiment, Ann. Geophys., 19, 1303–1354, 2001, http://www.ann-geophys.net/19/1303/2001/.

Roux, A., Perraut, S., Robert, P., Morane, A., Pedersen, A., Korth, A., Kremser, G., Aparicio, B., Rodgers, D., and Pellinen, R.: Plasma sheet instability related to the westward traveling surge, J. Geophys. Res., 96, 17 697–17 714, 1991.

Roux, A., Le Contel, O., Fontaine, D., Robert, R., Louarn, P., Sauvaud, J.-A., and Fazakerley, A. N.: Substorm theories and Cluster multi-point measurements, in: Proceedings of the Eight International Conference on Substorms, edited by: Syrjasuo, M. and Donovan, E., pp. 263–268, University of Calgary, Calgary, Canada, 2006.

Saito, Y., Mukai, T., Terasawa, T., Nishida, A., Machida, S., Hirahara, M., Maezawa, K., Kokubun, S., and Yamamoto, T.: Slow-mode shocks in the magnetotail, J. Geophys. Res., 100, 23 567–23 582, 1995.

Schödel, R., Nakamura, R., Baumjohann, W., and Mukai, T.: Rapid flux transport and plasma sheet reconfiguration, J. Geophys. Res., 106, 8381–8390, 2001.

Semenov, V. S., Heyn, M. F., and Ivanov, I. B.: Magnetic reconnection with space and time varying reconnection rates in a compressible plasmas, Phys. Plasmas, 11, 62–70, 2004.

Sergeev, V., Elphic, R. C., Mozer, F. S., Saint-Marc, A., and Sauvaud, J.-A.: A two-satellite study of nightside flux transfer events in the plasma sheet, Planet. Space Sci., 40, 1551–1572, 1992.

Sergeev, V. A., Angelopoulos, V., Mitchell, D. G., and Russell, C. T.: In situ observations of magnetotail reconnection prior to the onset of a small substorm, J. Geophys. Res, 100, 19 121–19 134, 1995.

Sergeev, V. A., Kubyshkina, M. V., Baumjohann, W., Nakamura, R., Amm, O., Pulkkinen, T., Angelopoulos, V., Mende, S. B., Klecker, B., Nagai, T., Sauvaud, J.-A., Slavin, J. A., and Thomsen, M. F.: Transition from substorm growth to substorm expansion phase as observed with a radial configuration of ISTP and Cluster spacecraft, Ann. Geophys., 23, 2183–2198, 2005, http://www.ann-geophys.net/23/2183/2005/.

Shirataka, N., Fujimoto, M., Hasegawa, H., and TanDokoro, R.: Reproducing the bi-polar magnetic signature at the jet leading edge by 3-D reconnection with non-zero guide field, J. Geophys. Res., 111, A07201, doi:10.1029/2005JA011521, 2006.

Slavin, J. A., Lepping, R. P., Gjerloev, J., Fairfield, D. H., Hesse, M., Owen, C. J., Moldwin, M. B., Nagai, T., Ieda, A., and Mukai, T.: Geotail observations of magnetic flux ropes in the plasma sheet, J. Geophys. Res., 108, 1015, doi:10.1029/2002JA009557, 2003.

Sonnerup, B. U. Ö. and Scheible, M.: Minimum and maximum variance analysis, in: Analysis Methods for Multi-Spacecraft Data, edited by: Paschmann, G. and Daly, P., pp. 185–220, ESA, Noordwijk, 1998.

Sonnerup, B. U. Ö., Paschmann, G., Papamastorakis, I., Sckopke, N., Haerendel, G., Bame, S. J., Asbridge, J. R., Gosling, J. T., and Russell, C. T.: Evidence for magnetic field reconnection at the earth's magnetopause, J. Geophys. Res., 86, 10 049–10 067, 1981.

Treumann, R. A., Jaroschek, C. H., Nakamura, R., Runov, A., and Scholer, M.: The role of the Hall effect in collisionless magnetic reconnection, Adv. Space. Res., 38, 101–111, 2006.

Voronkov, I., Runov, A., Koustov, A., Kabin, K., Meurant, M., Donovan, E., Bryant, C., and Spanswick, E.: Features of magnetosphere-ionosphere coupling during breakups and substorm onsets inferred from multi-instrument alignment, in: Proceedings of the Eght International Conference on Substorms, edited by: Syrjasuo, M. and Donovan, E., pp. 319–324, University of Calgary, Calgary, Canada, 2006.

Voronkov, I. O.: Near-Earth breakup triggered by the earthward traveling burst flow, Geophys. Res. Lett., 32, L13107, doi: 10.1029/2005GL022983, 2005.

Xiao, C. J., Wang, X. G., Pu, Z. Y., Zhao, H., Wang, J. X., Ma, Z. W., Fu, S. Y., Kivelson, M. G., Liu, Z. X., Zong, Q. G., Glassmeier, K. H., Balogh, A., Korth, A., Rème, H., and Escoubet, C. P.: In situ evidence for the structure of the magnetic null in a 3D reconnection event in the Earth's magnetotail, Nature Physics, 2, 478–483, doi:10.1038/nphys342, 2006.

Zong, Q.-G., Fritz, T. A., Pu, Z. Y., Fu, S. Y., Baker, D. N., Zhang, H., Lui, A. T., Vogiatzis, I., Glassmeier, K.-H., Korth, A., Daly, P. W., Balogh, A., and Rème, H.: Cluster observations of earthward flowing plasmoid in the tail, Geophys. Res. Lett., 31, L18803, doi:10.1029/2004GL020692, 2004.